Aiguo Xing · Xiaoyi Yuan · Qiang Xu · Qihua Zhao · Heqing Huang · Qiangong Cheng

Characteristics and numerical runout modelling of a catastrophic rock avalanche triggered by the Wenchuan earthquake in the Wenjia valley, Mianzhu, Sichuan, China

Abstract The 2008 Wenchuan earthquake triggered more than 100 rock avalanches with volumes greater than 10 million cubic metres. The rock avalanche with the longest runout amongst these destructive landslides occurred in the Wenjia valley, Mianzhu, Sichuan, China. The landslide involved the failure of about 27.5 million cubic metres of sandstone from the source area. The displaced material travelled about 4,170 m with an elevation descent of about 1,360 m, equivalent to a fahrböschung of 16.9° and covered an area of 1.5 million square metres, with the final deposited volume of approximately 49 million cubic metres. The catastrophic event destroyed the village of Yanjing, killed 48 people and buried some houses at the mouth of the Wenjia valley. On the basis of a detailed field investigation, we introduce basic characteristics of the rock avalanche and find that the rock avalanche resulted in two run-ups and a superelevation along the runout path, and downslope enlargement due to the entrainment of path materials. A numerical model (DAN3D) is used to simulate the post-failure behaviour of the rock avalanche. By means of trial and error, a combination of the frictional model and Voellmy model is found to provide the best performance in simulating this rock avalanche. The simulation results reveal that the rock avalanche had a duration of about 240 s and an average velocity of 17.4 m/s.

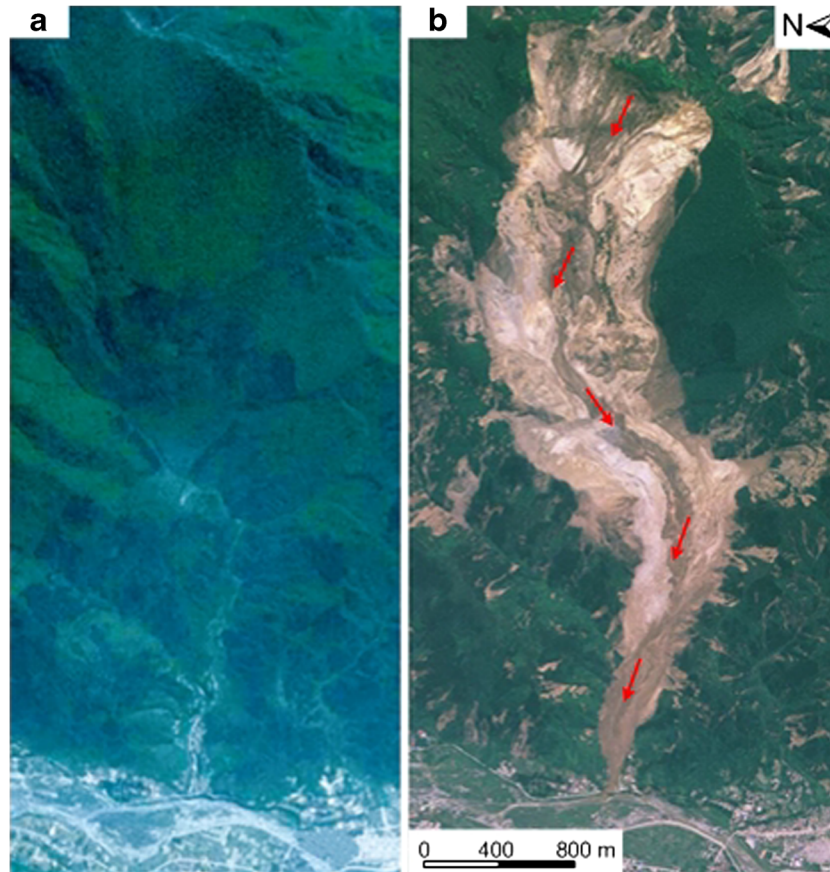**Keywords** Rock avalanche · Post-failure behaviour · Numerical modelling · DAN3D model · Wenchuan earthquake

Introduction

Southwestern China is located at the southeastern margin of the Tibetan Plateau and corresponds to a region of high seismic activity (Chen et al. 2012). Historical records show that strong earthquakes have triggered many landslides and caused significant damage (Weidinger et al. 2002; Dai et al. 2005; Cui et al. 2009; Yin et al. 2009). At 14:28 (Beijing time) on 12 May 2008, the Wenchuan earthquake (M_s = 8.0) struck in the Longmenshan fault zone, Sichuan, China. This region is characterized by high relief with a deeply incised valley. Long-duration seismic shaking triggered a number of landslides within the epicentral and surrounding regions (Yin et al. 2009; Chigira et al. 2010; Dai et al. 2011; Gorum et al. 2011; Huang and Fan 2013; Xu et al. 2014). The large volume of landslide material deposited on the slopes in the region enabled the occurrence of numerous post-seismic debris flows, resulting in the further loss of lives and extensive damage to many newly constructed towns and facilities (Parker et al. 2011; Tang et al. 2012; Zhang et al. 2014a). These geohazards killed more than 20,000 people, nearly a quarter of the total of 87,000 deaths resulting from the earthquake (Yin et al. 2009).

However, catastrophic rock avalanches are amongst the most destructive landslides triggered by the Wenchuan earthquake, and remote sensing interpretation showed that the earthquake triggered more than 100 rock avalanches with volumes greater than 10 million cubic metres (Huang et al. 2011). There has been much research on the rock avalanches triggered by this seismic event (e.g. Wang et al. 2009, 2013, 2015; Qi et al. 2011; Yin et al. 2011; Huang et al. 2012a; Yin 2014; Tang et al. 2015; Zhang et al. 2015). Several numerical simulations have analysed the runout behaviours of the rock avalanches triggered by the earthquake (Huang et al. 2012b; Li et al. 2012; Zhang et al. 2013; Zhou et al. 2013; Zhu et al. 2013; Dai et al. 2014; Yuan et al. 2014; Xing et al. 2015; Yin et al. 2015). These simulations have investigated the sliding process of landslide materials originating from the source area. Nevertheless, some rock avalanches involved not only the movement of debris originating from the landslide source area but also the movement of runout path materials and, in some cases, entrainment of material along the runout path which, in some cases, greatly enlarged the landslide volume and elevated the mobility of the displaced landslide material (Chigira et al. 2010; Wang et al. 2013). For example, a large rock avalanche (located at latitude 31°33′04.7″ N and longitude 104°06′58.5″ E) was triggered by the Wenchuan earthquake in the village of Yanjing, Mianzhu City, Sichuan Province, southwestern China (hereinafter called Wenjia valley rock avalanche). The displaced material travelled about 4,170 m with an elevation descent of about 1,360 m, equivalent to a fahrböschung of 16.9°, less than other landslides with this volume (Huang et al. 2011), and covered an area of 1.5 million square metres, with the final deposited volume of approximately 49 million cubic metres. The displaced landslide material destroyed Yanjing, killed 48 people and buried some houses at the mouth of the Wenjia valley (Fig. 1).

Much research has focused on the rainfall-induced secondary debris flows of the catastrophic event (Tang et al. 2009; Ni et al. 2012; Xu et al. 2012; Zhang et al. 2013, 2014b; Van Asch et al. 2014; Zhou and Tang 2014). Five main debris flows occurred in the Wenjia valley from 24 September 2008 to 18 September 2010. However, little attention has been paid to the post-failure behaviour and debris characteristics of the landslide. Zhang et al. (2016) examined the dynamics of the Wenjia valley rock avalanche through field and laboratory investigations and remote sensing. The results show that shear resistance between grains decreased as the grains became finer due to pervasive fragmentation, which is one of the possible mechanisms by which the granular debris was able to travel a long distance at a high speed. Understanding the characteristics and also the possible movement of this kind of landslide is important to future landslide hazard mitigation. Therefore, a detailed field investigation of the Wenjia valley rock avalanche was performed to allow discussion of the geological and climatic setting and examination of the main characteristics of the landslide.

Fig. 1 Pre-event image in Google Earth from 12 April 2006 (*left*) and post-event aerial image taken on 18 May 2008 (*right*) of the Wenjia valley rock avalanche

Understanding the triggering mechanism and post-failure behaviour of such rock avalanches is a challenge in geosciences and a prerequisite for the future prevention or mitigation of disasters. Many numerical studies have been performed to better understand the landslide runout behaviour, and some rational approaches have been proposed for predicting the motion of landslide masses (e.g. Sassa 1988; Hungr 1995; Chen and Lee 2003; Crosta et al. 2003; Denlinger and Iverson 2004; Hungr and Evans 2004; McDougall and Hungr 2004; Poisel et al. 2008; Pirulli and Mangeney 2008; Huang et al. 2012b; Pudasaini and Miller 2013; Pastor et al. 2014; Delaney and Evans 2015). Although the effectiveness of these approaches has been validated by back-analyses of many landslides, the successful forecasting of landslide movement has been rarely reported because different models or parameters of these approaches should be used for different types of landslides. However, back-analyses of case histories are essential because successful back-analyses may be used to calibrate the models, improve forecasting accuracy and provide parameters specific to similar types of rapid landslides for use in the predictive modelling of potential landslides. The present project numerically analysed the post-failure behaviour of the Wenjia valley rock avalanche using the dynamic model DAN3D, which was developed by Hungr and his colleagues (McDougall and Hungr 2004). This model is based on the numerical solutions of depth-averaged shallow-water equations, which have been modified for the flow of earth materials. This model relates to a meshless numerical

method, based on smoothed particle hydrodynamics, and allows the simulation of motion across real three-dimensional topography without the mesh distortion problem, and it is thus suitable for the back-analysis of fluidized landslides. Smoothed particle hydrodynamics models combined with depth-integrated equations have been developed and extended to simulate the propagation stage of flow-like landslides, debris flows, lahars and avalanches (McDougall and Hungr 2004; Pastor et al. 2009; Haddad et al. 2010; Huang and Dai 2014). DAN3D allows the simulation of a catastrophic event through systematic iteration of the parameters that govern the basal resistance until the characteristics of the simulated landslide (i.e. velocity, extent and depth of deposits) approximately match those of the real event (McDougall and Hungr 2005). Through the numerical analysis of the Wenjia valley rock avalanche, the most suitable rheological models and parameters were calibrated and validated according to the results of the field investigation. It is expected that these models and parameters will help clarify the propagation process of similar landslides and improve the accuracy of landslide hazard mapping in the region.

Geological and geographical setting

The Wenjia valley is situated near the town of Qingping in the Mianzhu county, in Sichuan. The valley is located on the left bank of the Mianyuan River, about 80 km northeast of the epicentre of the Wenchuan earthquake (Tang et al. 2012). The Wenjia valley landslide occurred in a region of low-mid relief with a moderately

incised valley. The elevations range from 2,402 m at the summit of Mount Jiudingshan to 883 m at the mouth of the Wenjia valley (Fig. 2). The depth of the valley incision ranges from 30 to 50 m, the longitudinal gradient of the valley bottom ranges from 150 to 180 ‰, and the angle of the side slope ranges from 35° to 55°.

The exposed rocks in the study area include the Guanwushan Group limestone of the Upper Devonian and the Qingping Group siltstone of the Upper Cambrian. The Guanwushan Group overlaps on the Qingping Group and there is nonconformity between them. The landslide is a dip slope failure that occurred in the Guanwushan Group. According to a pre-event Google Earth image and eyewitness reports, the source rock mass was stable before the earthquake.

The study area has a humid subtropical monsoon climate. The average annual temperature is about 14.4 °C and the annual rainfall ranges from 1500 to 1700 mm in Qingping. The maximum daily rainfall recorded was 496.5 mm on 15 August 1995, according to the historical record of this area for the last several decades. There are many streams and well-developed water systems, all of which belong to the Tuo River. The Mianyuan River, a tributary of the Tuo River, has a length of 63.5 km and an average yearly discharge of 15.7 m³/s. The Wenjia valley is located on the left bank of the Mianyuan River. The valley has a length of 3 km and a drainage area of 7.8 km².
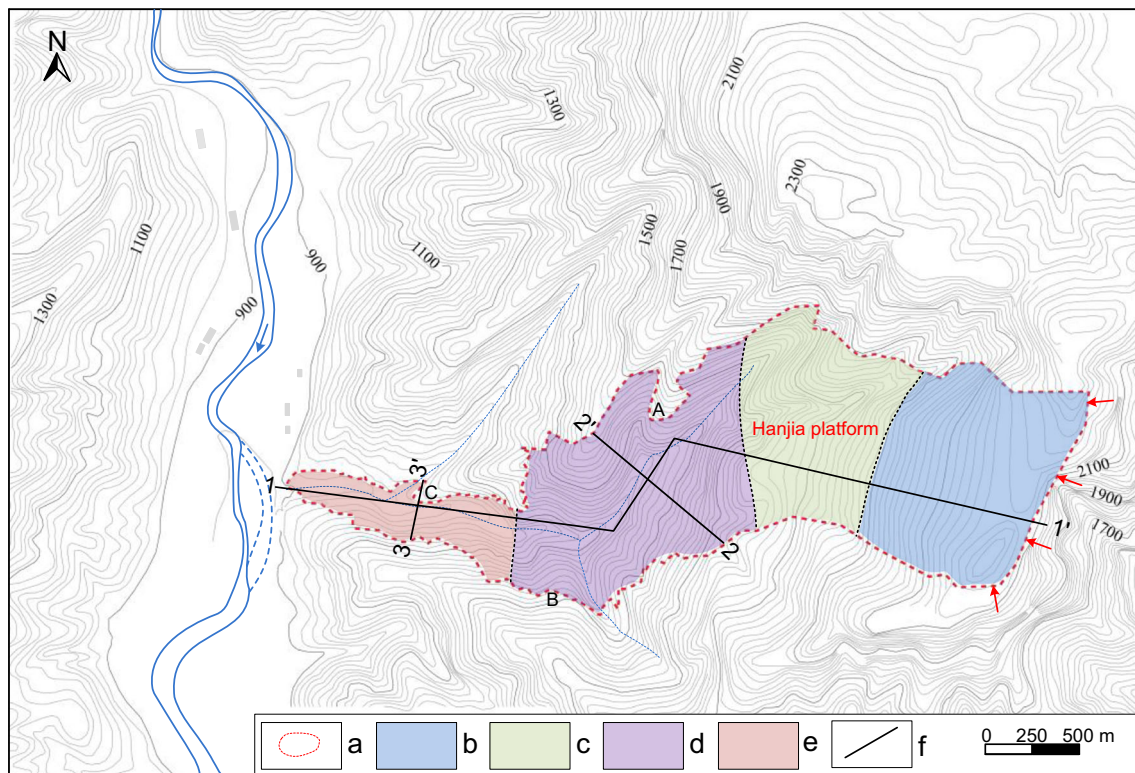
Wenjia valley rock avalanche

Post-failure behaviour of the rock avalanche
On the basis of a detailed field investigation, a geological map and longitudinal profile of the Wenjia valley rock avalanche are presented in Figs. 2 and 3, respectively. The landslide initiated as a

rock slide in the limestone rock mass. After detaching from its source area under strong earthquake ground motions, the sliding mass on the left side ran down rapidly towards the direction of 283° and then transformed into debris flow as it impacted the Hanjia platform. After passing a scarp with a height of about 280 m at an elevation of 1599 m, the debris ran up the opposite slope on the right bank of the valley at location A in Fig. 2. After colliding with the right bank of the valley (Fig. 4a), the debris flow changed its direction and entered the platform at an elevation of 1300 m at a direction of 123°. The debris flow superelevated at the valley bend (Fig. 4b, c) at location B in Fig. 2. The debris changed direction again and travelled down along the valley at a direction of 278° and then ran up the ridge with a trend of 070° at location C in Fig. 2. After colliding with the right bank of the valley (Fig. 4d), the debris continued to move along the valley at a direction 278° west of south and finally came to rest at the mouth of the valley. The displaced materials created an air blast so powerful that it downed trees along its sides and front margin, indicating the rapid movement of the rock avalanche (Fig. 5).

Detailed description of the rock avalanche
The source area is located on the eastern slope of the Wenjia valley, 3.6 km from the Yingxiu-Beichuan Fault, which caused the Wenchuan earthquake. The head scarp and toe of the rupture surface are at elevations of 2268 and 1780 m, respectively. This area has a length of 960 m along the main slide direction, a width of 500–1080 m and an area of 0.69 km² (Fig. 6a). The sliding mass mainly consisted of Upper Devonian Guanwushan limestone with a thickness of 20–30 m and an initial volume of 28.5 million cubic

Fig. 2 Detailed topography of the Wenjia valley rock avalanche. *a* Landslide boundary. *b* Source area. *c* Hanjia platform (zone I). *d* Zone II. *e* Zone III. *f* Cross-section line. *Red arrows* express the sliding direction of the sliding mass
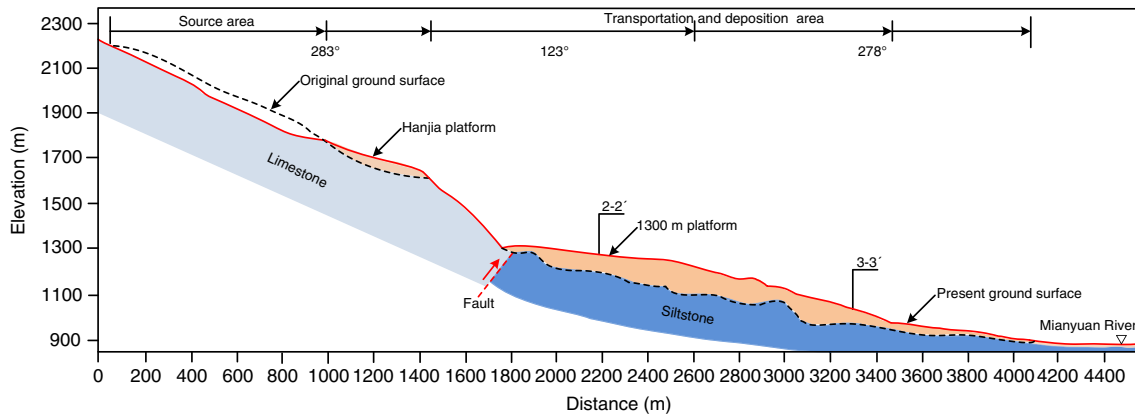
Fig. 3 Longitudinal profile of the Wenjia valley rock avalanche along line 1-1′ shown in Fig. 2

metres. Three major joint sets are present at 315°/70° (J1), 135°/38° (J2) and 237°/78° (J3) and the bedding plane is 320°/32° (Fig. 6b). The sliding surface developed along the bedding plane (Fig. 6c).

The displaced materials were mainly deposited at elevations ranging from 908 to 1780 m. The area of transportation and deposition can be divided into three zones according to the elevation, direction of the landslide motion and longitudinal gradient of the deposits (Fig. 2). The grain size distribution of the deposits is shown in Table 1.

Zone I is located at the Hanjia platform between the toe of the source area and the scarp and has elevations ranging from 1599 to 1780 m (Fig. 7a). This subzone has a volume of 22.6 million cubic metres (Xu et al. 2012) and a longitudinal channel gradient of 10–30°. The slide mass entrained the original Quaternary deposit on the Hanjia platform and damaged part of a fir tree forest on the left side of the zone (Fig. 7b). The landslide deposits in this zone consist of poorly sorted debris and its parent rock is limestone. The rock avalanche debris contains 30 % particles larger than 100 cm, 40 % particles ranging in size from 20 to 100 cm, 20 % particles ranging in size from 1 to 20 cm and 10 % particles smaller than 1 cm in diameter.

Zone II is located between the cliff (Fig. 7a) and the mouth of the right branch of the Wenjia valley and has elevations ranging from 988 to 1400 m (Fig. 2). The zone includes two subzones (zones IIa and IIb), according to the direction of the landslide motion.

Zone IIa is located at the 1300-m platform along the direction of 123° and has elevations ranging from 1225 to 1400 m (Fig. 7a). This subzone has an average longitudinal gradient of about 5° and a thickness greater than 100 m. Three longitudinal ridges can be found in this subzone. The first ridge is on the left side of the valley and has a trend of 203°, a length of 270 m and a width of 34 (Fig. 8). The rock avalanche debris deposited on the ridge contains 5 % particles larger than 20 cm, 20 % particles ranging in size from 1 to 20 cm and 75 % particles smaller than 1 cm in diameter. The second ridge is also on the right side of the valley resulting from the run-up at location A in Fig. 2 and has a trend of 220°, a length of 550 m and a maximum width of 160 m (Figs. 7c and 8). The rock avalanche debris deposited on the ridge contains 10 % particles larger than 20 cm, 60 % particles ranging in size from 1 to 20 cm and 30 % particles smaller than 1 cm in diameter;

the largest boulder is more than 160 cm in diameter. The third ridge is on the left side of the valley and results from the superelevation at location B in Fig. 2 and has a strike of 240°, a length of 340 m and a width of 65 m (Fig. 7d). The rock avalanche debris deposited on the ridge contains 30 % particles larger than 100 cm, 25 % particles ranging in size from 20 to 100 cm, 30 % particles ranging in size from 1 to 20 cm and 15 % particles smaller than 1 cm in diameter.

Zone IIb is located at elevations ranging from 988 to 1225 m a.m.s.l. This subzone has an average longitudinal gradient of 18–25° and a thickness of 45–120 m. The rock avalanche debris deposited on the right side of the subzone contains 5 % particles larger than 100 cm, 25 % particles ranging in size from 20 to 100 cm, 40 % particles ranging in size from 1 to 20 cm and 30 % particles smaller than 1 cm in diameter. The rock avalanche debris deposited on the left side of the subzone contains less than 5 % particles larger than 100 cm, 10 % particles ranging in size from 20 to 100 cm, 35 % particles ranging from 1 to 20 cm and 40 % particles smaller than 1 cm in diameter.

Zone III is located at elevations ranging from 908 to 1016 m. Two platforms are found in this zone. The first platform is located at elevations of 988–1016 m and has an average longitudinal gradient of 5°, a length of 118 m and a width of 71 m (Fig. 7e). The rock avalanche debris deposited on the first platform contains 30 % particles ranging in size from 1 to 20 cm and 70 % particles smaller than 1 cm in diameter. The second platform is located at elevations of 908–988 m and has an average longitudinal channel gradient of about 6°, a length of 167 m and a width of 94 m (Fig. 7f). The platform has been covered by a secondary debris flow.

Numerical runout modelling of the rock avalanche

Dynamic model

Dynamic back-analysis can be empirical, using historical data such as those of the volume, fall height and runout (e.g. Scheidegger 1973; Corominas 1996), and/or numerical modelling to analyse the runout behaviour of the rock avalanche (Hungr et al. 2005). To investigate the runout behaviour of the Wenjia valley rock avalanche and provide parameters specific to the same type of

Fig. 4 Dynamic characteristics of the Wenjia valley rock avalanche. **a** Displaced materials ran up the opposite slope on the right bank of the valley at location *A* in Fig. 2 (view towards NWW). **b**, **c** Superelevation in the valley bend at location *B* in Fig. 2 (view towards 205° and 188°, respectively). **d** Run-up on the ridge with a trend 070° at location *C* in Fig. 2 (view towards 100°)
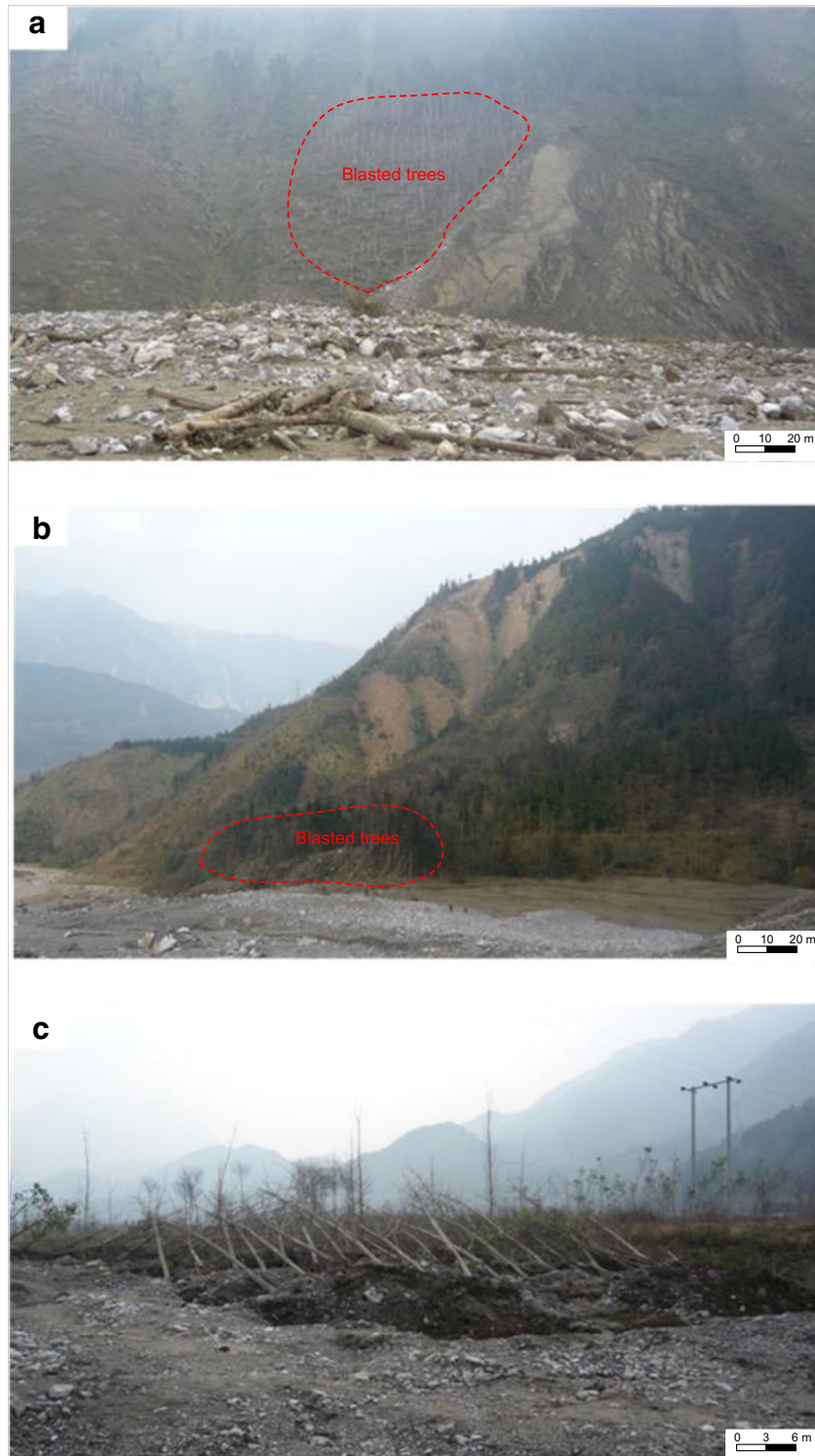
Fig. 5 Air blast downed trees along its sides and front margin. **a** On the left side of the valley (view towards 290°). **b** On the right side of the valley (view towards 290°). **c** On the right bank of the Mianyuan River (view towards 265°)

landslides for use in predictive modelling of potential landslides, the rock avalanche was numerically modelled using the dynamic model DAN3D developed by Hungr and his colleagues (McDougall and Hungr 2004).

The dynamic model is governed by internal and basal rheological relationships. The rheologies that have been found to represent recorded events most accurately are the frictional and Voellmy rheologies (Boultbee 2005). The frictional rheology
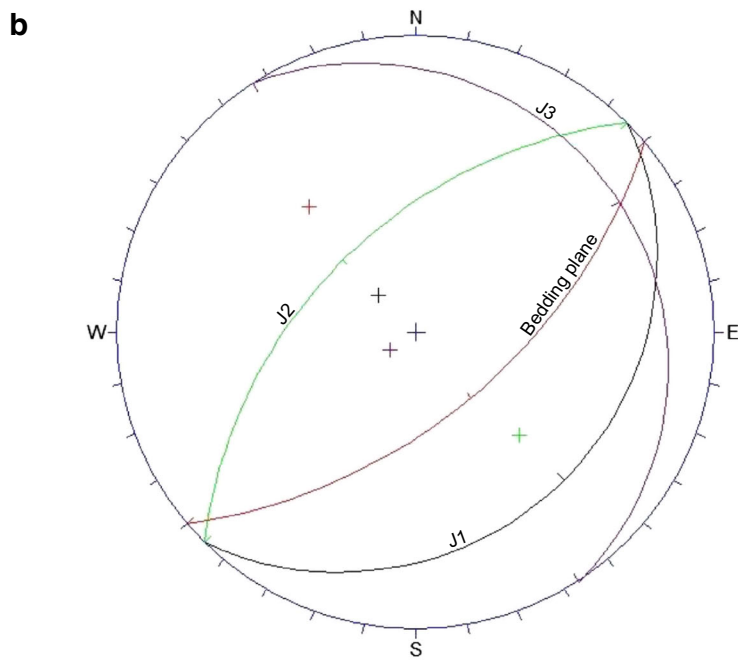
Fig. 6 **a** Source area of the Wenjia valley rock avalanche (view towards NEE). **b** Stereonet of the main discontinuity sets present in the source area, J1:315°/70°, J2:135°/38°, J3:237°/78°; the bedding plane is 320°/32°. **c** Cliff in the middle part of the source area

Table 1 Grain size distribution of the deposits in the different zones

		>100 cm	20–100 cm	1–20 cm	<1 cm
Zone I		30 %	40 %	20 %	10 %
Zone IIa	First ridge	5 % larger than 20 cm		20 %	75 %
	Second ridge	10 % larger than 20 cm		60 %	30 %
	Third ridge	30 %	25 %	30 %	15 %
Zone IIb	Right side	5 %	25 %	40 %	30 %
	Left side	5 %	10 %	35 %	40 %
Zone III	First platform			30 %	70 %

assumes the resisting shear force (τ) to depend only on the effective normal stress (σ). The frictional equation is expressed as

$$\tau = \sigma(1-r_u)\tan\phi \tag{1}$$

where the pore pressure ratio, r_u, and the dynamic friction angle, ϕ, are the rheological parameters to be introduced in the model. The pore pressure ratio is derived from the pore pressure, u, normalized by the total bed normal stress at the base, σ. The pore pressure ratio and the dynamic friction angle can be alternatively expressed by a single variable referred to as the bulk basal friction angle, ϕ_b:

$$\phi_b = \arctan(1-r_u)\tan\phi \tag{2}$$

The Voellmy rheology describes total resistance as a sum of a frictional term and a turbulent term:
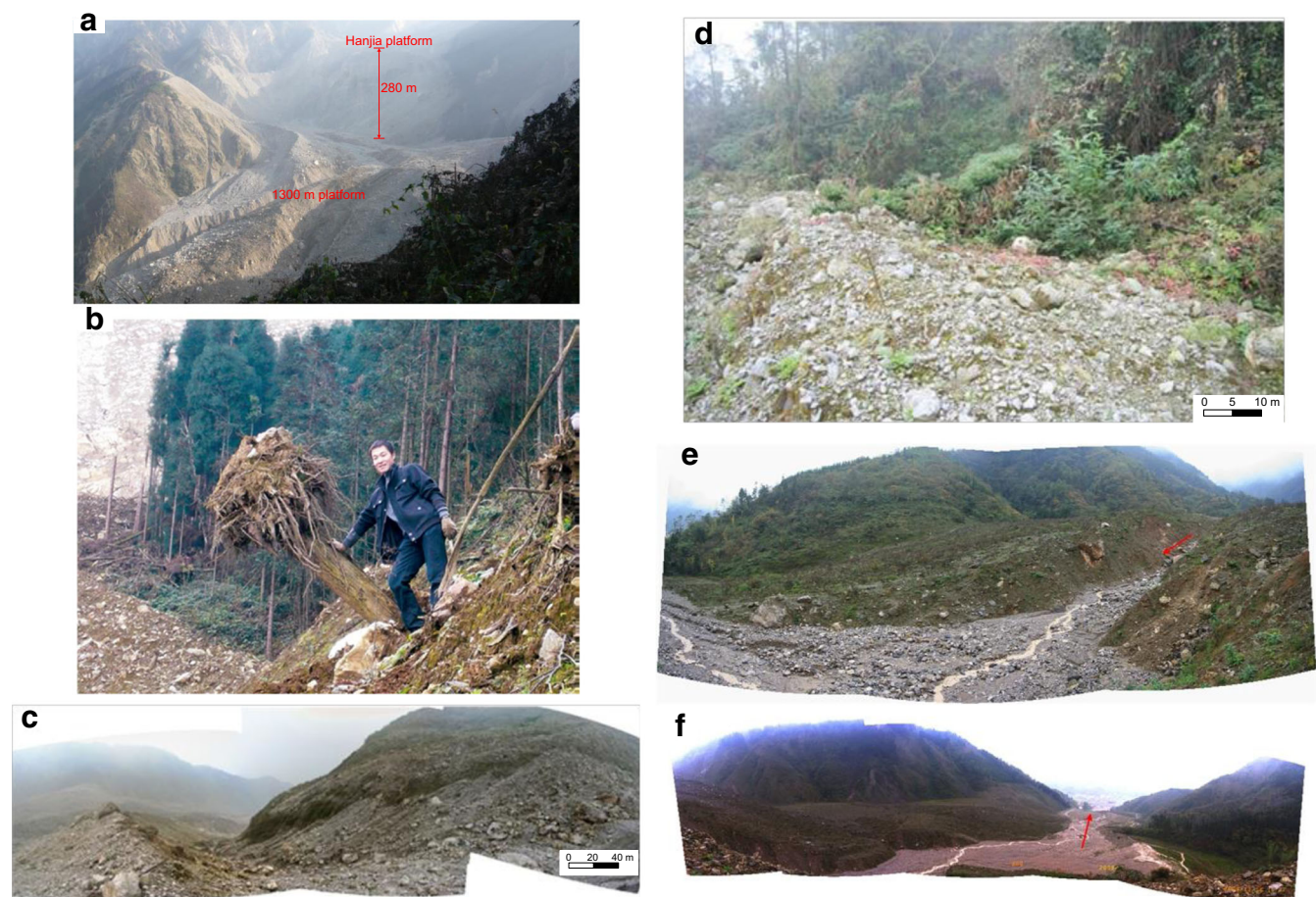
Fig. 7 Transportation and deposition area. **a** View of the Hanjia platform towards the source area (view towards 75°). **b** Damaged part of a fir tree forest on the left side of zone I (view towards NEE). **c** First run-up zone and longitudinal ridge (view towards NWW). **d** Longitudinal ridge on the left side of the valley resulting from the superelevation (view towards E). **e** First platform (view towards E). **f** Second platform (view towards 270°)
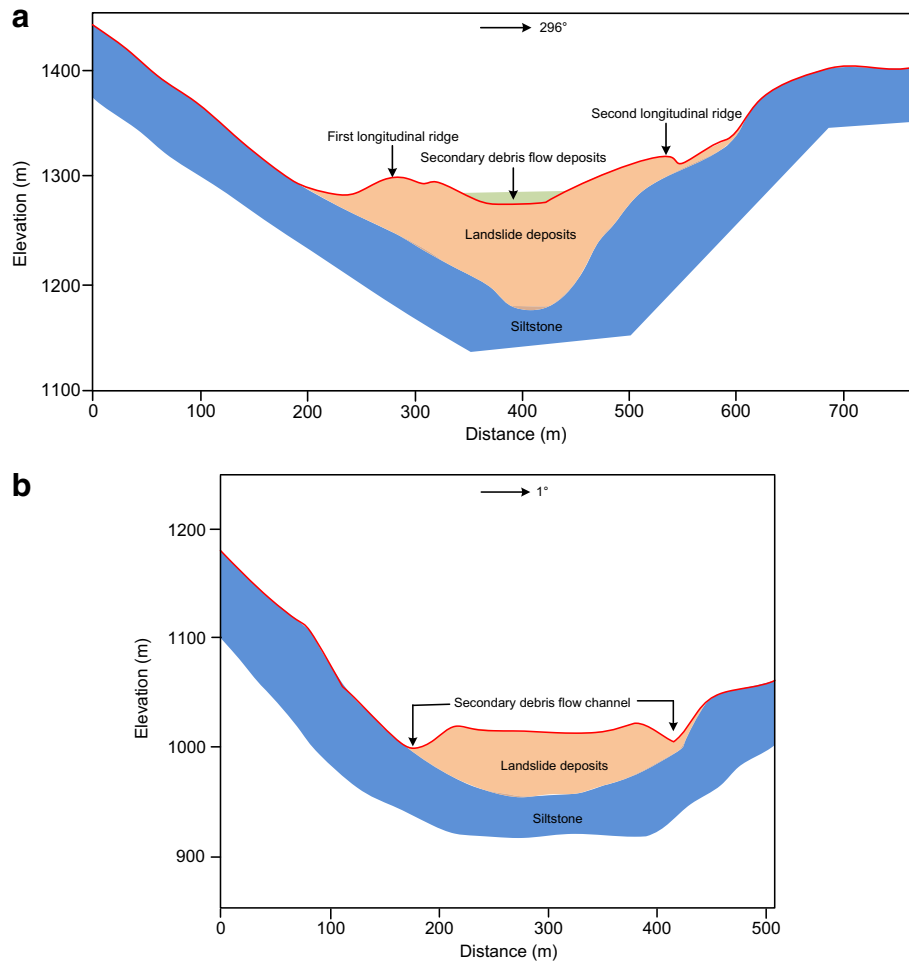
Fig. 8 Cross sections taken along lines 2-2′ (**a**) and 3-3′ (**b**) shown in Fig. 2

$$\tau = \sigma f + \rho g v^2 / \xi \qquad (3)$$

The frictional term relates the shear stress to the normal stress through a friction coefficient, f, which is analogous to $\tan\phi_b$. The turbulent term summarizes all velocity-dependent factors of flow resistance and is expressed by the square of the velocity and the density of the debris through a turbulence coefficient, ξ (Table 2).

Simulations of velocity were compared to the estimation of velocity from run-up and superelevation. The run-up velocity was obtained as (Evans et al. 2001)

$$V_{\min} = (2gh)^{0.5} \qquad (4)$$

where $V_{\min}$ (in metres per second) is the minimum velocity, g is the gravitational constant and h is the run-up height.

The superelevation velocity was estimated as (Evans et al. 2001)

$$V_{\min} = (gdr/b)^{0.5} \qquad (5)$$

where d is the superelevation, r is the radius of curvature of the bend and b is the width of the path.

Input data

The pre- and post-DEMs (digital elevation models) were created by superimposing the 1:50,000-scale pre-event topographic map on the post-event aerial image (Fig. 9). The input sliding surface and source thickness files were created using pre- and post-event DEMs at a scale of 1:50,000. The source depths were approximated by subtracting the post-event DEM from the pre-event DEM and isolating the probable main failure zone. Data outside of this zone were filtered, leaving a displaced volume of approximately 28.5 million cubic metres. The isolated source depths were then subtracted from the pre-event DEM to estimate the initial sliding surface elevations. Assuming a volume of 25 % volume bulking, as suggested by Hungr and Evans (2004), the initial volume of displaced materials was estimated to be 35.6 million cubic metres for DAN3D simulation. Data spacing was set to 20 m for input into the model.

The model has several parameters, including both control and rheological parameters (McDougall and Hungr 2004). The control parameters are the number of particles, N; the particle smoothing coefficient, B; the velocity smoothing coefficient, C; and the stiffness coefficient, D. The rheological parameters are the internal friction angle, ϕ_i, the basal rheological parameters (which depend on the selected basal rheology) and, if applicable, the entrainment growth rate, E_s.

Table 2 Back-calculated values of the rheological parameters and models for the Wenjia valley rock avalanche

|	Rheology	ϕ (deg)	r_u	f	ξ (m/s^2)
Source area	Frictional	30.0	0.62	–	–
Zone I	Frictional	30.0	–	–	–
Zones II and III	Voellmy	–	–	0.09	2000

Continuum simulation is performed through discretization of the governing equations, but a sufficiently large number of computational elements (particles) are required to capture the behaviour at each important location within the sliding mass. Increasing the number of particles (N) can increase the resolution of the continuum method. The particle smoothing coefficient (B) affects the smoothness of the interpolated flow depth, and it can be adjusted by the user until the initial depth interpolation appears smooth. The velocity smoothing coefficient (C) determines how much the velocities of neighbouring particles affect the central particle. Velocity smoothing introduces some numerical diffusion, which appears to smooth out strong shocks, increase stability and reduce the tendency for particles to line up in the downstream direction in channelized reaches of the path. The dimensionless stiffness coefficient (D) controls the strain-dependent rate of the transition between the active and passive internal stress states. On the basis of the parametric analyses presented in this paper, the control parameters $N = 2000$, $B = 4$, $C = 0.45$ and $D = 460$ are recommended for the duration of motion.

In accordance with the equivalent fluid concept, a frictional model rheology was adopted to simulate the internal rheology of the slide mass. The yield criterion is governed by the internal friction angle (ϕ_i) and the effect of pore pressure can be accounted for implicitly with the internal friction angle. In this paper, an internal friction angle of 35° is set for the moving mass, without pore pressure in all simulations.

The frictional model can be used in the source area and zone I and the Voellmy rheology in zones II and III. The basal rheological parameters were adjusted by trial and error to achieve the best fit with the observed extension of the landslide deposit, considering also published values for comparable case studies (Hungr and Evans 1996; McDougall et al. 2006; Evans et al. 2007; Sosio et al. 2008). The transition between the frictional and Voellmy models was placed at an elevation of 1400 m. To the Donghekou rock

avalanche triggered by the 2008 Wenchuan earthquake, Wang et al. (2013) found that the sliding liquefaction phenomenon can occur on the landslide material in the source area during the main shock of the earthquake as a result of undrained shearing in a saturated sliding zone. Wang et al. (2014a, b) also performed the undrained cyclic shear tests and found that the monitored excess pore water pressure showed a delayed response—it reached a constant pore water pressure of 280 kPa under an estimated normal stress of 300 kPa—resulting in an effective normal stress of 20 kPa, indicating that this runout path material is highly liquefiable. Based on the above results, in order to simulate the frictional loss along the sliding surface resulting from the undrained loading, we examined excess pore water pressure acting on the potential sliding surface in the source area because soil in the sliding zone was fully saturated (equivalent to a range of the pore pressure ratio (r_u) of 0.5–0.8). A dynamic friction angle of 30° was adopted for the frictional model at zone I without buildup of pore pressure. A Voellmy rheology was selected to characterize the runout behaviour of the landslide below an elevation of 1400 m in zones II and III. For the simulation of this part of the path, values for the friction coefficient (f) in the range of 0.05–0.25 together with values for the turbulence coefficient (ξ) in the range of 100–2000 m/s^2 were used. It is noted that these values for the Voellmy parameters are within the range of those found to best simulate the runout and velocity of the majority of rockslide debris avalanche case histories analysed by Hungr and Evans (1996). These values were then used in a series of simulation runs to obtain the best fit for the observed characteristics of the Wenjia valley rock avalanche.

Mass and momentum transfer during the entrainment of the path material can affect landslide dynamics. A useful preliminary estimate of the average volume growth rate ($\overline{E_s}$) for a specific entrainment zone can be obtained using the natural exponential growth equation (McDougall and Hungr 2005):

a

b
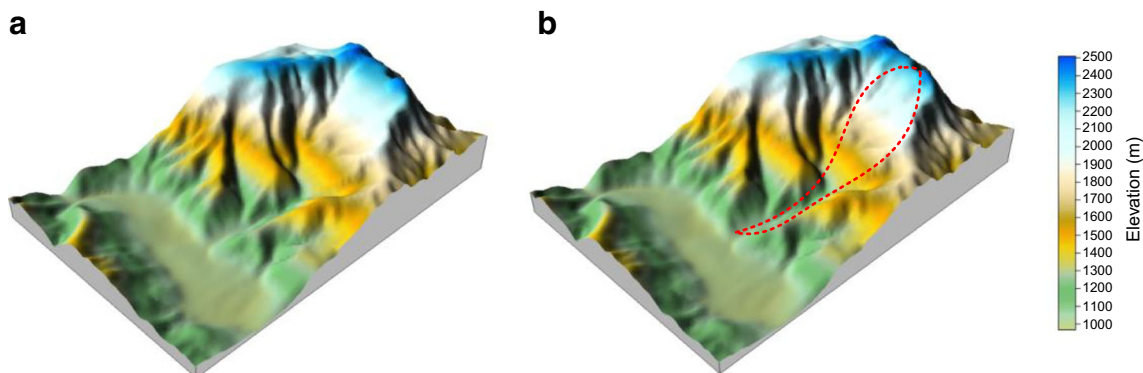
Fig. 9 Pre-event (**a**) and post-event (**b**) DEMS
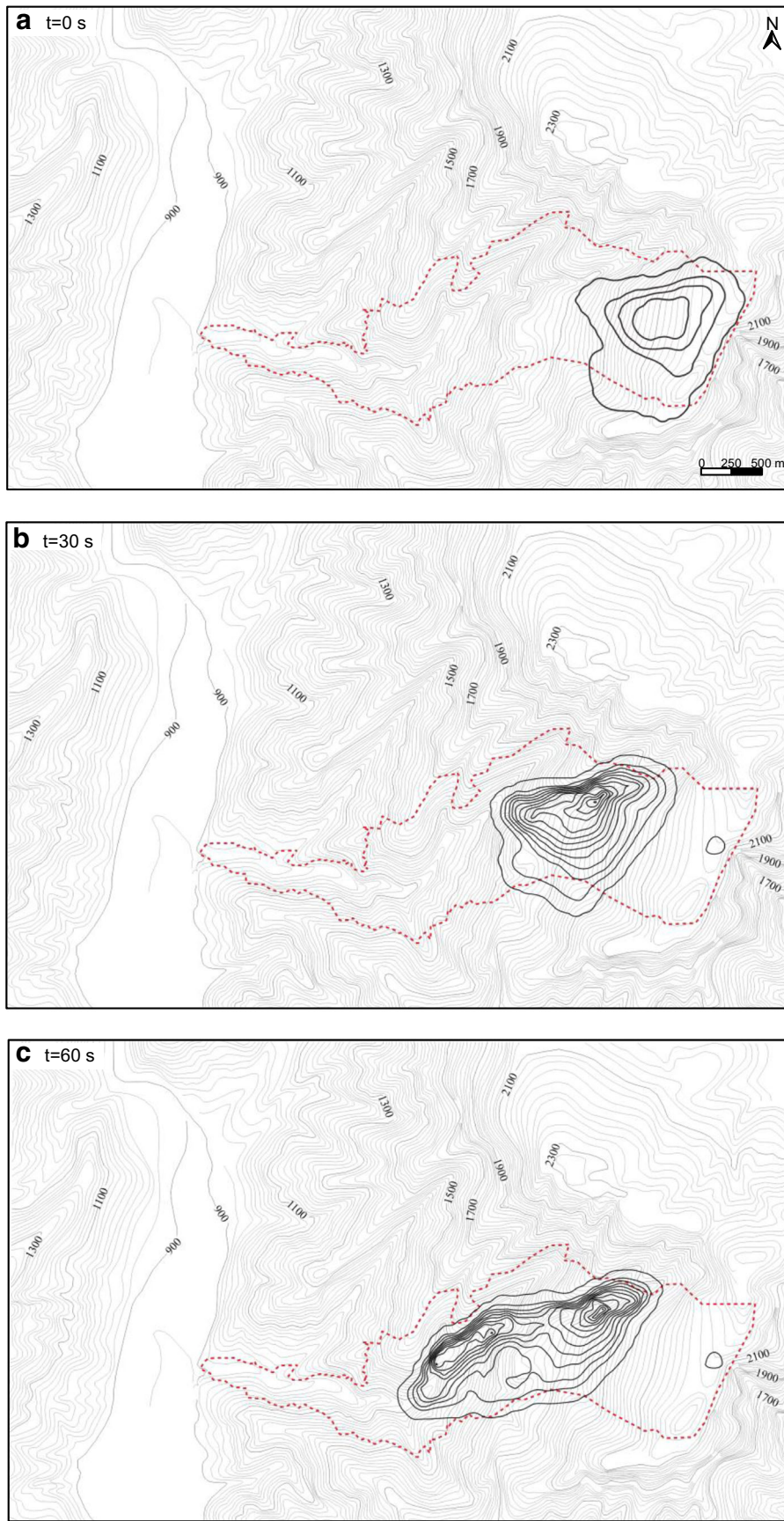
Fig. 10 a–i Time-lapse images of the DAN3D simulation. The contours of deposit depth are at 10-m intervala. The elevation contours are at 20-m intervals
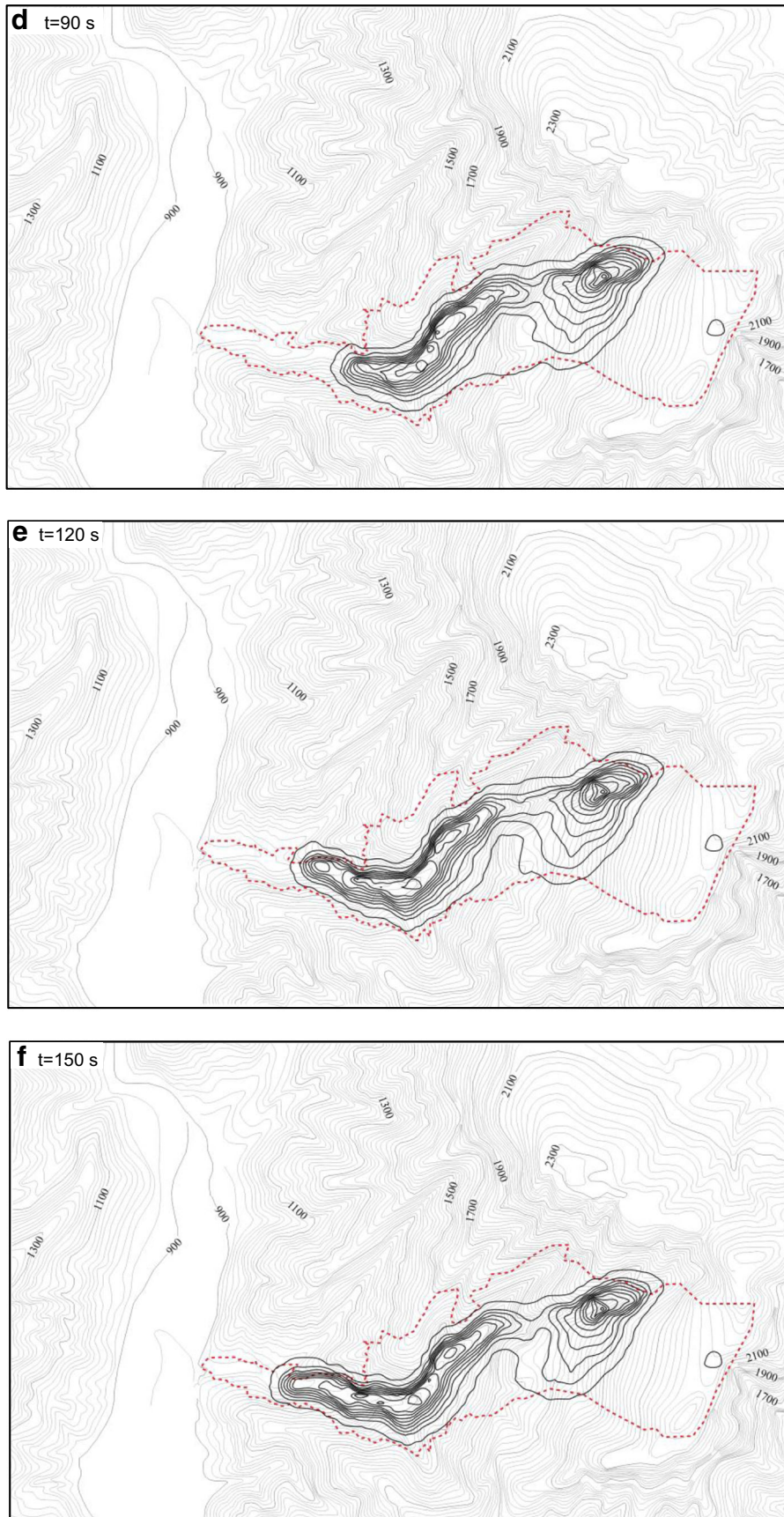
d t=90 s

e t=120 s

f t=150 s

Fig. 10 (continued)

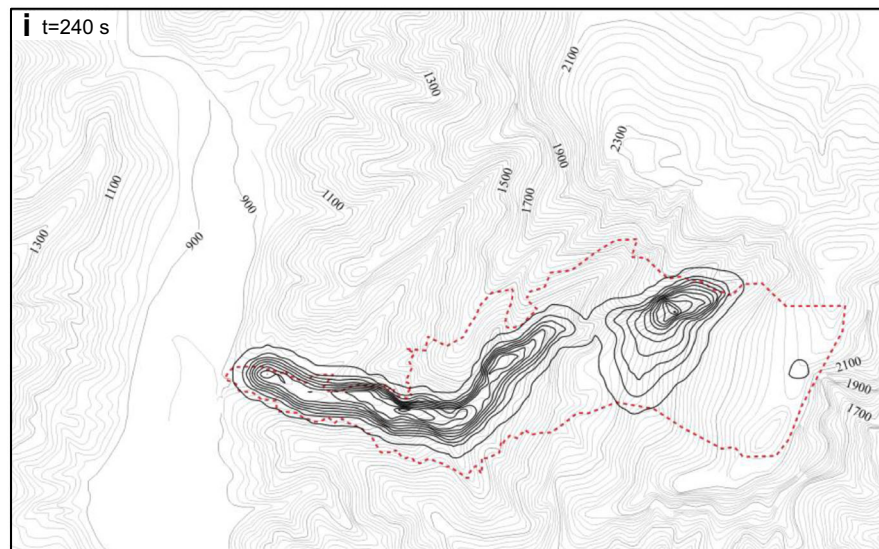**g** t=180 s
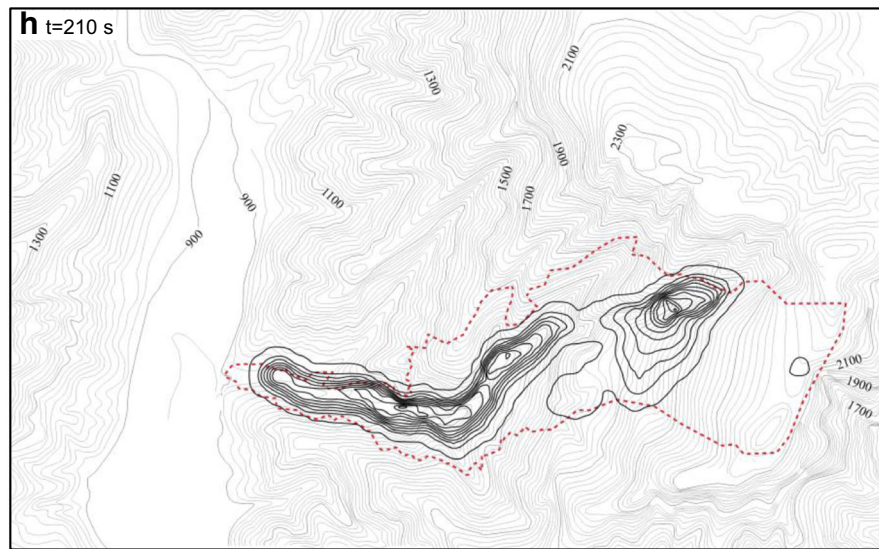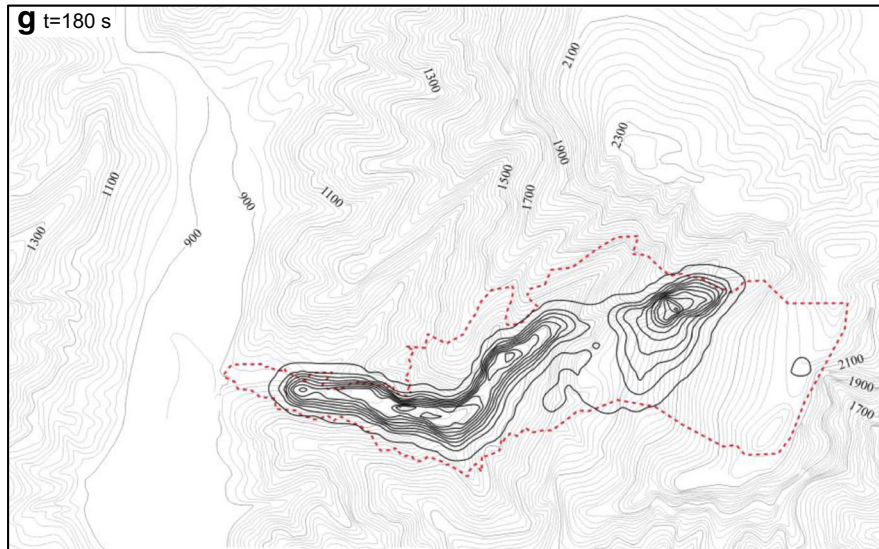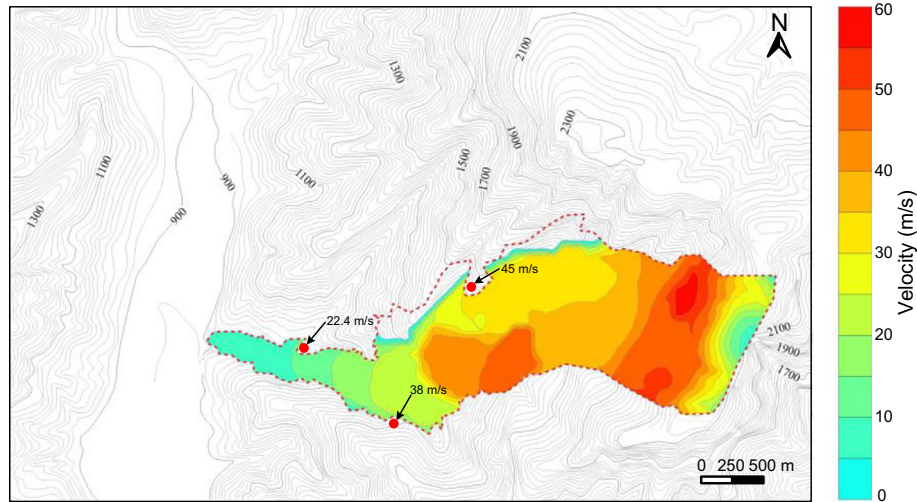

h t=210 s

i t=240 s

Fig. 10 (continued)

Fig. 11 Plot of the maximum simulated flow velocities recorded along the runout path. The maximum velocity contours are at 5-m/s intervals and the elevation contours are at 20-m intervals

$$V_f = V_o \exp\left(\overline{E_s \overline{S}}\right) \tag{6}$$

where V_f is the estimated total volume of the landslide exiting the zone, V_o is the estimated total volume of the landslide entering the zone and $\overline{S}$ is the approximate average path length of the zone. Given the initial and final volumes, as observed, and the approximate length of the entrainment zone, the appropriate rate to use in a simulation can be back-calculated using Eq. 6, which ensures that the required volume is entrained from the known length of the entrainment zone (cf. McDougall and Hungr 2005). To simulate entrainment, volume growth rates of 3.4×10^{-4} and 7.6×10^{-5} m^{-1} were specified at zones I, II and III, respectively.

Results and discussion

A series of back-analyses were performed to determine the best rheological parameters for the simulation (Table 1). The results of the DAN3D simulation are presented in Fig. 10. The runout is precisely duplicated with a dynamic friction angle (ϕ) of 30° and a

pore pressure ratio (r_u) of 0.62 for the materials in the source area, with a dynamic friction angle of 30° in zone I and with Vollemy parameters of friction coefficient $f = 0.09$ (dimensionless) and turbulent coefficient $\xi = 2,000$ m/s² in zones II and III. The results show that the duration of the movement is estimated at 240 s for an average velocity of 17.4 m/s. The simulated run-ups and superelevations in the three major impact zones match the measured trimline, suggesting that the flow velocities are accurately simulated.

A plot of the maximum simulated flow velocities recorded along the runout path is shown in Fig. 11. The maximum velocity, 56 m/s, was recorded near the toe of the rupture surface. As mentioned above, the possible velocities were also calibrated by means of run-ups and superelevations. After passing the cliff at an elevation of 1599 m, the debris ran up the opposite slope on the right bank of the valley at location A in Fig. 2, and Eq. 4 yields a velocity estimate of 45 m/s for a measured run-up of $h = 100$ m. The debris flow superelevated at the valley bend at location B in Fig. 2. For this bend, Eq. 5 yields a velocity of 38 m/s for the parameters of $d = 180$ m, $r = 600$ m and $b = 750$ m. The debris ran up the ridge at location C in
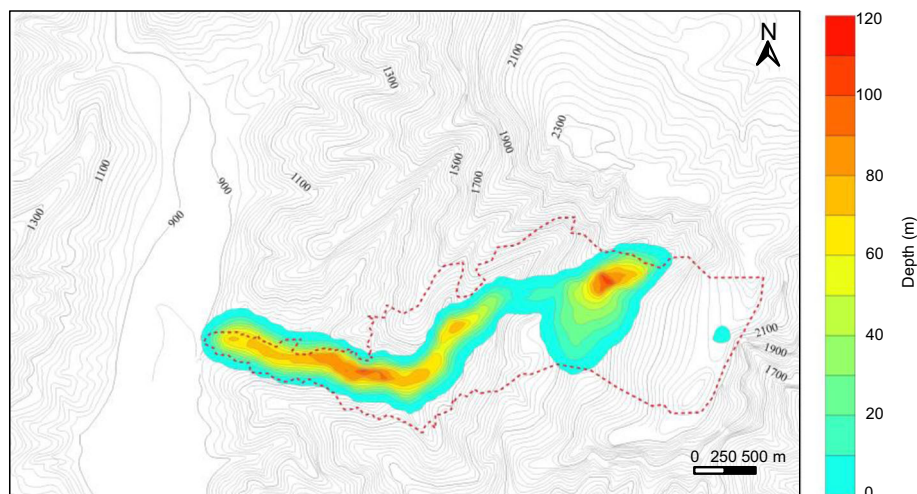
Fig. 12 Final distribution of the debris at 10-m intervals

Fig. 2, and Eq. 4 yields a velocity estimate of 22.4 m/s for a measured run-up of $h = 25$ m. Figure 10 shows that the simulated velocities are lower than the velocities from the results of the run-up and superelevation analysis. The differences in the velocities can be attributed to measurement errors associated with Eqs. 4 and 5, and determining the run-up height and radius of a curve from an aerial view is subject to limitations. It was thus difficult to match the DAN3D-simulated velocity values with the field velocities inferred from debris behaviour.

The final distribution of the debris obtained in the simulation is shown in Fig. 12. The figure gives an average depth of about 43 m and a maximum depth of over 112 m at the Hanjia platform; these results are roughly consistent with the range of the depth obtained from the DEMs constructed from 1:50,000-scale topographic maps. The final deposit volume was estimated to be 49.0 million cubic metres due to entrainment along the runout path.

Using the DAN3D model, many case studies of rapidly moving landslides in North America have been analysed and a valuable database of calibrated parameters has been created (cf. Hungr et al. 2005). We numerically modelled the Niumian valley rock avalanche triggered by the Wenchuan earthquake using the DAN3D model (Xing et al. 2015). The simulated results show that the duration of the Niumian valley rock avalanche is about 120 s with an average velocity of 22 m/s, and the Wenjiagou valley rock avalanche has a duration of about 240 s with an average velocity of 17.4 m/s. The travel angle, fahrböschung, value of the Wenjia valley rock avalanche is less than that of the Niumian valley rock avalanche. Further case studies will be investigated using the DAN model to obtain rheological parameters for landslide hazard assessment in the mountainous areas of southwestern China.

Summary and conclusions

On 12 May 2008, the Wenjia valley rock avalanche was triggered by the Wenchuan earthquake in Mianzhu, Sichuan, China. On the basis of the field investigation, this paper introduced the general setting and main characteristics of the landslide and analysed the runout behaviour with the DAN3D model. The following summarizes the study.

1. The Wenjia valley rock avalanche was a rapid and long-runout catastrophic landslide triggered by the Wenchuan earthquake. This catastrophic event destroyed the village of Yanjing, killed 48 people and buried some houses at the mouth of the Wenjia valley. The displaced materials travelled about 4170 m, with a descent of about 1360 m.
2. A field investigation showed that the displaced materials created an air blast so powerful that it downed trees along its sides and front margin, indicating the rapid movement of the rock avalanche.
3. A recently developed dynamic model (DAN3D), which accounts for material entrainment along the runout path, was used to simulate the runout behaviour of this event. The sliding velocity and depositing area were modelled using a combined (Frictional–Frictional–Vollemy) model that well simulates the landslide.
4. The simulation results show that the rock avalanche had a duration of about 240 s and an average velocity of 17.4 m/s. The simulation velocities were lower than those obtained from the run-up and superelevation analysis. However, the simulation

predicted the shape of the deposit well. Good agreement between the observation and simulation results was achieved, suggesting that this model with the parameters obtained through back-analyses is useful for the prediction of landslides in the same area and similar types of landslide hazard.

References

Boultbee N (2005) Characterization of the Zymoetz River rock avalanche. MSc thesis, Simon Fraser University, Burnaby

Chen H, Lee CF (2003) A dynamic model for rainfall-induced landslides on natural slopes. Geomorphology 51(4):269–288

Chen XL, Ran HL, Yang WT (2012) Evaluation of factors controlling large earthquake-induced landslides by the Wenchuan earthquake. Nat Hazards Earth Syst Sci 12:3645–3657

Chigira M, Wu XY, Inokuchi T, Wang GH (2010) Landslides induced by the 2008 Wenchuan earthquake, Sichuan, China. Geomorphology 118(3–4):225–238

Corominas J (1996) The angle of reach as a mobility index for small and large landslides. Can Geotech J 33:260–271

Crosta GB, Imposimato S, Roddeman DG (2003) Numerical modelling of large landslides stability and runout. Nat Hazards Earth Syst Sci 3(6):523–538

Cui P, Zhu YY, Han YS, Chen XQ, Zhuang JQ (2009) The 12 May Wenchuan earthquake induced landslide lakes: distribution and preliminary risk evaluation. Landslides 6(3):209–223

Dai FC, Lee CF, Deng JH, Tham LG (2005) The 1786 earthquake-triggered landslide dam and subsequent dam-break flood on the Dadu River, southwestern China. Geomorphology 65(3–4):205–221

Dai FC, Xu C, Yao X, Xu L, Tu XB, Gong QM (2011) Spatial distribution of landslides triggered by the 2008 Ms 8.0 Wenchuan earthquake, China. J Asian Earth Sci 40(4):883–895

Dai ZL, Huang Y, Cheng HL, Xu Q (2014) 3D numerical modeling using smoothed particle hydrodynamics of flow-like landslide propagation triggered by the 2008 Wenchuan earthquake. Eng Geol 180(8):21–33

Delaney KB, Evans SG (2015) The 2000 Yigong landslide (Tibetan Plateau), rockslide-dammed lake and outburst flood: review, remote sensing analysis, and process modelling. Geomorphology 246:377–393

Denlinger RP, Iverson RM (2004) Granular avalanches across irregular three-dimensional terrain: 1. Theory and computation. J Geophys Res Earth Surf 109(F1):1–14

Evans SG, Hungr O, Clague JJ (2001) Dynamics of the 1984 rock avalanche and associated distal debris flow on Mount Cayley, British Columbia, Canada; implications for landslide hazard assessment on dissected volcanoes. Eng Geol 61:29–51

Evans SG, Guthrie RH, Roberts NJ, Bishop NF (2007) The disastrous 17 February 2006 rockslide-debris avalanche on Leyte Island, Philippines: a catastrophic landslide in tropical mountain terrain. Nat Hazards Earth Syst Sci 7:89–101

Gorum T, Fan XM, van Westen CJ, Huang RQ, Xu Q, Tang C, Wang GH (2011) Distribution pattern of earthquake-induced landslides triggered by the 12 May 2008 Wenchuan earthquake. Geomorphology 133(3–4):152–167

Haddad B, Pastor M, Palacios D, Munoz-Salinas E (2010) A SPH depth integrated model for Popocatepetl 2001 lahar (Mexico): sensitivity analysis and runout simulation. Eng Geol 114(3–4):312–329

Huang Y, Dai ZL (2014) Large deformation and failure simulations for geo-disasters using smoothed particle hydrodynamics method. Eng Geol 168:86–97

Huang RQ, Fan XM (2013) The landslide story. Nat Geosci 6(5):325–326

Huang RQ, Xu Q, Huo JJ (2011) Mechanism and geo-mechanics models of landslides triggered by 5.12 Wenchuan earthquake. J Mt Sci 8(2):200–210

Huang RQ, Pei XJ, Fan XM, Zhang WF (2012a) The characteristics and failure mechanism of the largest landslide triggered by the Wenchuan earthquake, May 12, 2008, China. Landslides 9:131–142

Huang Y, Zhang WJ, Xu Q, Xie P, Hao L (2012b) Run-out analysis of flow-like landslides triggered by the Ms 8.0 2008 Wenchuan earthquake using smoothed particle hydrodynamics. Landslides 9(2):275–283

Hungr O (1995) A model for the runout analysis of rapid flow slides, debris flows, and avalanches. Can Geotech J 32(4):610–623

Hungr O, Evans SG (1996) Rock avalanche run out prediction using a dynamic model. In: Senneset K (ed) Proceedings of the 7th International Symposium on Landslides, Trondheim 1, pp 233–238

Hungr O, Evans SG (2004) Entrainment of debris in rock avalanches: an analysis of a long run-out. Geol Soc Am Bull 116(9–10):1240–1252

Hungr O, McDougall S, Bovis M (2005) Entrainment of material by debris flows. In: Jakob M, Hungr O (eds) Debris flow hazards and related phenomena. Springer, Heidelberg, pp 135–158

Li XB, He SM, Luo Y, Wu Y (2012) Simulation of the sliding process of Donghekou landslide triggered by the Wenchuan earthquake using a distinct element method. Environ Earth Sci 65(4):1049–1054

McDougall S, Hungr O (2004) A model for the analysis of rapid landslide motion across three-dimensional terrain. Can Geotech J 41(6):1084–1097

McDougall S, Hungr O (2005) Dynamic modelling of entrainment in rapid landslides. Can Geotech J 42(5):1437–1448

McDougall S, Boultbee N, Hungr O, Stead D, Schwab JW (2006) The Zymoetz River landslide, British Columbia, Canada: description and dynamic analysis of a rock slide-debris flow. Landslides 3:195–204

Ni HY, Zheng WM, Bo TY, Su PC, Tang YQ, Xu RG (2012) Formation and characteristics of post-earthquake debris flow: a case study from Wenjia gully in Mianzhu, Sichuan, SW China. Nat Hazards 61(2):317–335

Parker RN, Densmore AL, Rosser NJ, de Michele M, Li Y, Huang RQ, Whadcoat S, Petley DN (2011) Mass wasting triggered by the 2008 Wenchuan earthquake is greater than orogenic growth. Nat Geosci 4(7):449–452

Pastor M, Haddad B, Sorbino G, Cuomo S, Drempetic V (2009) A depth-integrated, coupled SPH model for flow-like landslides and related phenomena. Int J Numer Anal Methods Geomech 33(2):143–172

Pastor M, Blanc T, Haddad B, Petrone S, Sanchez Morles M, Drempetic V, Issler D, Crosta GB, Cascini L, Sorbino G, Cuomo S (2014) Application of a SPH depth-integrated model to landslide run-out analysis. Landslides 11:793–812

Pirulli M, Mangeney A (2008) Results of back-analysis of the propagation of rock avalanches as a function of the assumed rheology. Rock Mech Rock Eng 41(1):59–84

Poisel R, Preh A, Hungr O (2008) Run out of landslides—continuum mechanics versus discontinuum mechanics models. Geomech Tunn 1(5):358–366

Pudasaini SP, Miller SA (2013) The hypermobility of huge landslides and avalanches. Eng Geol 157:124–132

Qi SW, Xu Q, Zhang B, Zhou YD, Lan HX, Li LH (2011) Source characteristics of long runout rock avalanches triggered by the 2008 Wenchuan earthquake, China. J Asian Earth Sci 40(4):896–906

Sassa K (1988) Geotechnical model for the motion of landslides. Proceedings of the 5th International Symposium on Landslides, "Landslides". Balkema, Rotterdam, vol 1 pp 37–56

Scheidegger AE (1973) On the prediction of the reach and velocity of catastrophic landslides. Rock Mech 5:231–236

Sosio R, Crosta GB, Hungr O (2008) Complete dynamic modeling calibration for the Thurwieser rock avalanche (Italian Central Alps). Eng Geol 100(1–2):11–26

Tang C, Zhu J, Li WL (2009) Rainfall-triggered debris flows following the Wenchuan earthquake. Bull Eng Geol Environ 68:187–194

Tang C, Van Asch TWJ, Chang M, Chen GQ, Zhao XH, Huang XC (2012) Catastrophic debris flows on 13 August 2010 in the Qingping area, southwestern China: the combined effects of a strong earthquake and subsequent rainstorms. Geomorphology 139–140:559–576

Tang YX, Zhang ZJ, Wang C, Zhang H, Wu F, Liu M (2015) Characterization of the giant landslide at Wenjiagou by the insar technique using TSX-TDX CoSSC data. Landslides 12:1015–1021. doi:10.1007/s10346-015-0616-z

Van Asch TWJ, Tang C, Alkema D, Zhu J, Zhou W (2014) An integrated model to assess critical rainfall thresholds for run-out distances of debris flows. Nat Hazards 70(1):299–311

Wang FW, Cheng QG, Highland L, Miyajima M, Wang HB, Yan CG (2009) Preliminary investigation of some large landslides triggered by the 2008 Wenchuan earthquake, Sichuan Province, China. Landslides 6(1):47–54

Wang GH, Huang RQ, Chigira M, Wu XY, Lourenco SDN (2013) Landslide amplification by liquefaction of runout-path material after the 2008 Wenchuan (M 8.0) earthquake, China. Earth Surf Process Landf 38(3):265–274

Wang FW, Sun P, Highland L, Cheng QG (2014a) Key factors influencing the mechanism of rapid and long runout landslides triggered by the 2008 Wenchuan earthquake, China. Geoenviron Disasters 1:1–16

Wang GH, Huang RQ, Lourenço SDN, Kamai T (2014b) A large landslide triggered by the 2008 Wenchuan (M8.0) earthquake in Donghekou area: phenomena and mechanisms. Eng Geol 182(Part B):148–157

Wang YF, Cheng QG, Zhu Q (2015) Surface microscopic examinations of quartz grains from rock avalanche basal travel zones. Can Geotech J 52:67–181

Weidinger JT, Wang JD, Ma NX (2002) The earthquake-triggered rock avalanche of Cui Hua, Qin Ling Mountains, P. R. of China—the benefits of a lake-damming prehistoric natural disaster. Quat Int 93–94:207–214

Xing AG, Xu Q, Gan JJ (2015) On characteristics and dynamic analysis of the Niumian valley rock avalanche triggered by the 2008 Wenchuan earthquake, Sichuan, China. Environ Earth Sci 73:3387–3401

Xu Q, Zhang S, Li WL, van Asch TWJ (2012) The 13 August 2010 catastrophic debris flows after the 2008 Wenchuan earthquake, China. Nat Hazards Earth Syst Sci 12:201–216

Xu C, Xu XW, Yao X, Dai FC (2014) Three (nearly) complete inventories of landslides triggered by the May 12, 2008 Wenchuan Mw 7.9 earthquake of China and their spatial distribution statistical analysis. Landslides 11(3):441–461

Yin YP (2014) Vertical acceleration effect on landsides triggered by the Wenchuan earthquake, China. Environ Earth Sci 71:4703–4714

Yin YP, Wang FW, Sun P (2009) Landslide hazards triggered by the 2008 Wenchuan earthquake, Sichuan, China. Landslides 6(2):139–152

Yin YP, Zheng WM, Li XC, Sun P, Li B (2011) Catastrophic landslides associated with the M8.0 Wenchuan earthquake. Bull Eng Geol Environ 70(1):15–32

Yin YP, Li B, Wang WP (2015) Dynamic analysis of the stabilized Wangjiayan landslide in the Wenchuan Ms 8.0 earthquake and aftershocks. Landslides 12(3):537–547

Yuan RM, Tang CL, Hu JC, Xu XW (2014) Mechanism of the Donghekou landslide triggered by the 2008 Wenchuan earthquake revealed by discrete element modeling. Nat Hazards Earth Syst Sci 14:1195–1205

Zhang YB, Chen GQ, Zhen L, Li YG, Wu J (2013) Effects of near-fault seismic loadings on run-out of large-scale landslide: a case study. Eng Geol 166:216–236

Zhang S, Zhang LM, Chen HX (2014a) Relationships among three repeated large-scale debris flows at the Pubugou Ravine in the Wenchuan earthquake zone. Can Geotech J 51(9):51–965

Zhang YS, Cheng YL, Yin YP, Lan HX, Wang J, Fu XX (2014b) High-position debris flow: a long-term active geohazard after the Wenchuan earthquake. Eng Geol 180:45–54

Zhang YB, Zhang J, Chen GQ (2015) Effects of vertical seismic force on initiation of the Daguangbao landslide induced by the 2008 Wenchuan earthquake. Soil Dyn Earthq Eng 73:91–102

Zhang M, Yin YP, McSaveney (2016) Dynamics of the 2008 earthquake-triggered Wenjiagou Creek rock avalanche, Qingping, Sichuan, China. Eng Geol 200:75–87

Zhou W, Tang C (2014) Rainfall thresholds for debris flow initiation in the Wenchuan earthquake-stricken area, southwestern China. Landslides 11(5):877–887

Zhou JW, Cui P, Yang YG (2013) Dynamic process analysis for the initiation and movement of the Donghekou landslide-debris flow triggered by the Wenchuan earthquake. J Asian Earth Sci 76:70–84

Zhu SB, Shi YL, Lu M, Xie FR (2013) Dynamic mechanisms of earthquake-triggered landslides. Sci China Earth Sci 56(10):1769–1779

A. Xing (✉) · **X. Yuan**
State Key Laboratory of Ocean Engineering,
Shanghai Jiao Tong University,
Shanghai, 200240, China
e-mail: xingaiguo@sjtu.edu.cn

Q. Xu · **Q. Zhao**
State Key Laboratory of Geohazard Prevention and Geoenvironment Protection,
Chengdu University of Technology,
Chengdu, 610059, China

H. Huang
Second Highway Consultant Co. Ltd,
China Communications Construction Company Limited,
Wuhan, 430056, China

Q. Cheng
Faculty of Geosciences and Environmental and Engineering,
Southwest Jiaotong University,
Chengdu, 610031, China